

Research Article www.acsami.org

Highly Stretchable, Tissue-like Ag Nanowire-Enhanced Ionogel Nanocomposites as an Ionogel-Based Wearable Sensor for Body **Motion Monitoring**

Siyuan Liu, Yizhang Wu, Lai Jiang, Wanrong Xie, Brayden Davis, Meixiang Wang, Lin Zhang, Yihan Liu, Sicheng Xing, Michael D. Dickey, and Wubin Bai*



Cite This: ACS Appl. Mater. Interfaces 2024, 16, 46538-46547



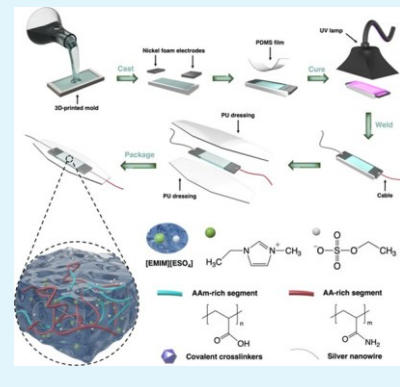
ACCESS

III Metrics & More

Article Recommendations

Supporting Information

ABSTRACT: The development of wearable electronic devices for human health monitoring requires materials with high mechanical performance and sensitivity. In this study, we present a novel transparent tissue-like ionogel-based wearable sensor based on silver nanowire-reinforced ionogel nanocomposites, P(AAm-co-AA) ionogel-Ag NWs composite. The composite exhibits a high stretchability of 605% strain and a moderate fracture stress of about 377 kPa. The sensor also demonstrates a sensitive response to temperature changes and electrostatic adsorption. By encapsulating the nanocomposite in a polyurethane transparent film dressing, we address issues such as skin irritation and enable multidirectional stretching. Measuring resistive changes of the ionogel nanocomposite in response to corresponding strain changes enables its utility as a highly stretchable wearable sensor with excellent performance in sensitivity, stability, and repeatability. The fabricated pressure sensor array exhibits great proficiency in stress distribution, capacitance sensing, and discernment of fluctuations in both external electric fields and stress. Our findings



suggest that this material holds promise for applications in wearable and flexible strain sensors, temperature sensors, pressure sensors, and actuators.

KEYWORDS: wearable sensors, ionogel, nanocomposite, stretchable sensors, ionogel sensors, mechanical sensors

INTRODUCTION

The development of wearable electronic devices with high mechanical performance and outstanding sensitivity is driven by the need to address human health monitoring and environmental concerns.^{1,2} Such devices in the form of flexible sensors,^{3–6} soft electronic skins,^{7,8} and textile electronics^{9–12} offer comfortable skin-interfaced compatibility. The practical applications of wearable electronic devices demand the designs to explore both unique structures (such as wavy structures, 13,14 kirigami structures, 15-17 serpentine meshes 18-20) and materials, including nanomesh,21,22 conductive or semiconductive polymers or composites, 23-26 and liquid metals. 27,28 Recently developed strategies for structural engineering and materials development have yielded significant benefits for advancing wearable performance, but significant limitations remain. For instance, thin-film circuits made of highly conductive metals have Young's modulus often over the MPa level, which is significantly higher than that of human tissues.²⁹ Also, conductive polymers and composites often face significant challenges related to poor solubility, biointerface compatibility, and poor dispersion and percolation,³⁰ which restrict their application in stretchable and wearable electronic devices.

Responsive gels with 3D polymeric networks solvated by small molecules are widely regarded as promising materials for

applications in wearable and stretchable devices with excellent sensing and actuation capabilities.^{31–33} Traditional responsive gels use water as the solvent to form hydrogels, which, however, often exhibit low conductivity,32,34 decreased mechanical property upon water evaporation in ambient environments, 35,36 limitations in modulating Young's modulus, and fabrication complexity. 37,38 Recently developed ionogels use ionic liquids (ILs) as the solvent, forming a composite system with high ionic conductivity, remarkable thermal stability, and a wide electrochemical window into the polymeric structure.36,39 For example, a photo-cross-linked ionogel based on dimethyl acrylamide-2-hydroxyethyl acrylate (DMA-HEA) network with IL, 3-hydroxyethyl-1-methylimidazolium dicyanamide, ([HMIm][DCA]) showed remarkable thermal stability (from −108 to 300 °C) with little change in the electrical and mechanical properties, as they are configured into wearable sensors.40

Received: June 26, 2024 July 22, 2024 Revised: Accepted: July 23, 2024 Published: August 1, 2024





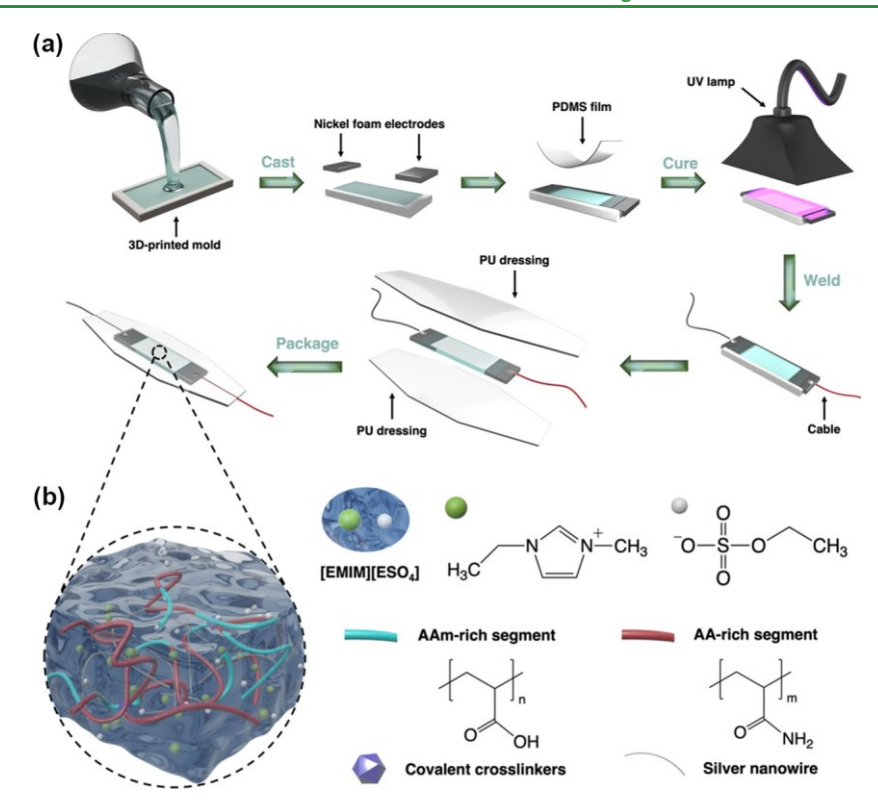


Figure 1. Synthesis of Ag NW-P(AAm-co-AA) ionogel composites. (a) Schematic illustration of the fabrication process of the highly stretchable, tissue-like strain sensor based on compositing P(AAm-co-AA) ionogel with Ag NWs. (b) Schematic illustration showing the composite network, where Ag NWs uniformly distribute among both hydrogen-bonded PAAm domains and highly solvated, soft PAA domains.

However, existing challenges for utilizing ionogels as skininterface sensing materials include leakage of ILs^{41–43} or absorption of moisture from the surrounding environment,44 possible skin irritation and toxicity of some ILs, 45,46 and mismatched Young's modulus (usually below 50 kPa or over 100 kPa for ionogels, whereas skin has Young's modulus ranging from 5 kPa to over 100 kPa). 41-43 To overcome the modulus mismatch, one effective way is to introduce nanofillers, such as nanoparticles, nanowires, and graphene into ionogels. For example, Zhang et al. developed an ionogel nanocomposite with high stretchability (2000%) and low Young's modulus that reaches 6.7–35.8 kPa, by doping with Fe₃O₄ nanoparticles into a loosely cross-linked ionogel network.^{47,48} Li et al. prepared a halloysite nanotube-enhanced ionogel nanocomposite that exhibits a high modulus of up to 26.7 MPa.⁴⁸ Lu et al. reported a graphene-enhanced doublenetwork ionogel electrolyte for strain sensing, with a modulus of 3.64 MPa and a breaking elongation of 217%.44 However, further enhancement of the sensitivity and detection range of the sensing signals through conductive fillers is seldom investigated for inherently conductive hydrogels or ionic gels. Herein, we report a transparent tissue-like wearable sensor based on a nanocomposite of silver nanowires (Ag NW) and poly(acrylamide-co-acrylic acid) (P(AAm-co-AA)) ionogel to enable high stretchability (605% strain, ca. 300% increase compared with that of the pristine ionogel), moderate stress (377 kPa), a sensitive response to changes of mechanical strain (up to 200 %, $\Delta R/R_0 \approx 12\%$) and temperature (up to 60 °C, $\Delta R/R_0 \approx 30\%$), and a pronounced electrostatic attraction. We show an easily accessible commercial polyurethane (PU) transparent film dressing applied to encapsulate the ionogel nanocomposite provides both excellent insulation performance

to prevent the skin irritation caused by the IL and strong adhesion between them to prolong the stability of the composite material over multidirectional stretching. All of these unique properties make it a promising material for wearable and flexible strain sensors, temperature sensors, and pressure sensors, as demonstrated through benchtop and onbody tests. The ionogel-Ag NW composite holds great promise in advanced wearable sensors that can accommodate both high stretchability and tissue-like softness.

RESULTS AND DISCUSSION

Figure 1a shows the schematic process for the synthesis and fabrication of ionogel-nanowire composites. First, a mixture containing acrylic acid (AA) and acrylamide (AAm) monomers, N,N'-methylenebis(acrylamide) (MBAA) as a cross-linker, irgacure 2959 (I2959) photoinitiator, 1-ethyl-3methylimidazolium ethyl sulfate ([EMIM][ESO₄]) as the ionic liquid (IL), and Ag NWs (0.2%v/v) was poured into a 3Dprinted mold. Next, nickel (Ni) foam electrodes were placed on both sides of the mold, respectively, and covered with a polydimethylsiloxane (PDMS) film to ensure a smooth surface and uniform thickness. The mixture was then cured under an ultraviolet (UV) lamp. After curing, the PDMS film was removed and copper cables were soldered onto the two Ni foam electrodes. Finally, the ionogel nanocomposite strain sensor was packaged with PU transparent dressings. The preparation of ionogel matrix follows a previously reported method to ensure optimized toughness and stretchability.49 The ionogel-gold nanowires (Au NWs) composite and the ionogel-graphene oxide (GO) composite follow a similar fabrication process, except the Ag NWs are replaced with Au NWs and GO, respectively. More details are given in the

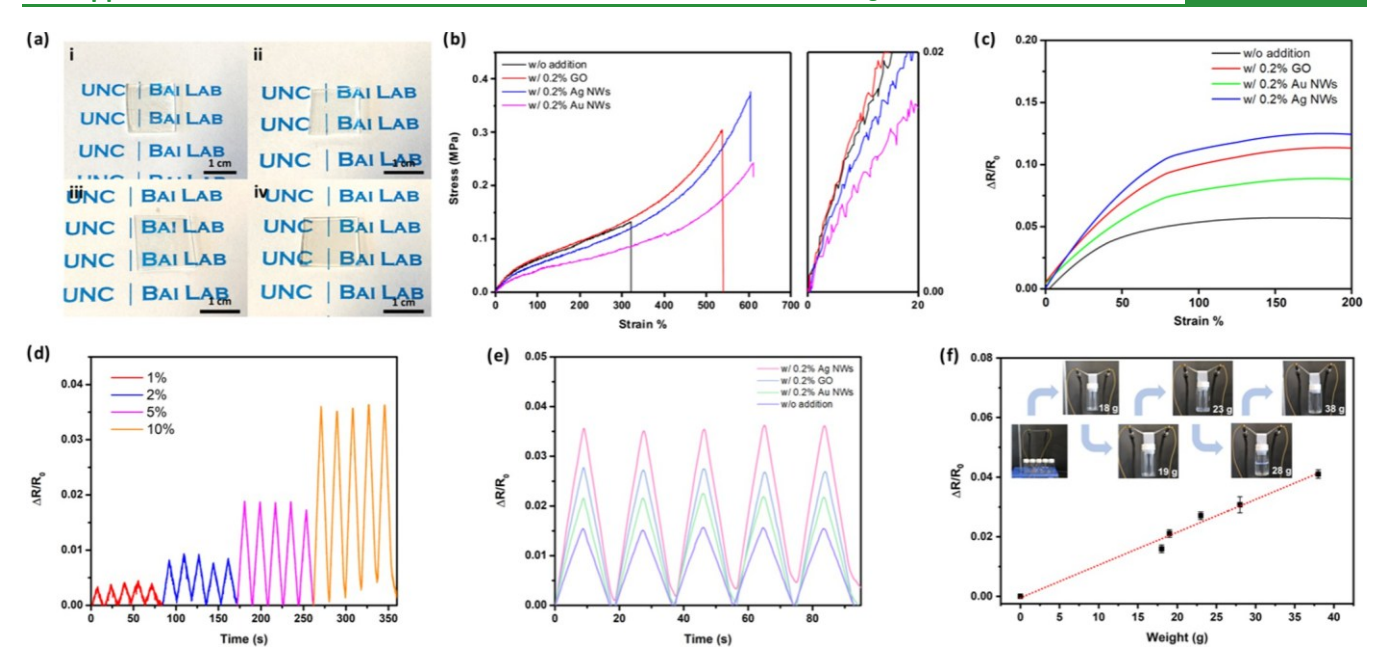


Figure 2. Mechanical and electrical properties of ionogel nanocomposites. (a) Optical images of P(AAm-co-AA) ionogel (i) without the addition of nanofillers, with the addition of (ii) 0.2% Ag NWs, (iii) 0.2% Au NWs, and (iv) 0.2% GO. (b) Measured stress—strain curves of pure P(AAm-co-AA) ionogel and P(AAm-co-AA) ionogel nanocomposites with various nanofillers. (c) Measured resistive change ($\Delta R/R_0$) of a slab (47.5 mm \times 15 mm \times 0.4 mm, length \times width \times thickness) of P(AAm-co-AA) ionogel nanocomposite as a function of strain. (d) Measured resistive change ($\Delta R/R_0$) of a slab (47.5 mm \times 15 mm \times 0.4 mm, length \times width \times thickness) of Ag NWs ionogel composite as a function of small strains (1, 2, 5, and 10%). (e) Measured resistive change ($\Delta R/R_0$) of P(AAm-co-AA) ionogel nanocomposites as a function of time during 5 stretch-release cycles under 10% strain. (f) Measured resistive change ($\Delta R/R_0$) of a slab (47.5 mm \times 15 mm \times 0.4 mm, length \times width \times thickness) of Ag NWs ionogel composite as a function of various weight loads (up to 39 g).

Supporting Information. Figure 1b illustrates the structural arrangement of the ionogel nanocomposites, where the acrylic acid-rich (AA-rich) segments and acrylamide-rich (AAm-rich) segments are highly cross-linked and entangled with the silver nanowires.^{50,51} The scanning electron microscopy (SEM) images depicting the morphology of the individual nanofillers (Ag NWs, Au NWs, and GO) prior to their incorporation into the ionogel matrix are shown in Figure S13a-c. The transmittance spectra for the P(AAm-co-AA) ionogel and its nanocomposites with various nanofillers, covering wavelengths from 300 to 1000 nm, are presented in Figure S14. Notably, even upon the introduction of nanofillers, the nanocomposites with Ag NWs and Au NWs as fillers exhibit a similar level of transparency to that of the intrinsic ionogel. This can be attributed to the effective dispersion of the nanofillers within the ionogel matrix, resulting in the formation of nanoscale networks that facilitate the passage of light.⁵²

The optical image of the Ag NW ionogel nanocomposites in Figure 2a shows good optical transparency, confirming the homogeneous dispersion and entanglements of the Ag NW with the P(AAm-co-AA) polymer networks. The Ag NW ionogel nanocomposites exhibit a distinct enhancement in stretchability and tensile strength. Figure 2b shows the stressstrain curves of three different ionogel nanocomposites as well as the pure ionogel as a reference. After adding nanofillers, both stress and strain show a significant increase. Particularly, the P(AAm-co-AA) ionogel with the addition of Ag NWs (0.2%v/v) shows an increase in strain at failure from 320 to 605%, compared with that of the pure ionogel without any additives. It suggests that the Ag NWs fillers can enable enhanced mechanics in conductive ionogels with a very small amount of filling, featuring low-cost scalability. The fracture strength of the Ag NWs ionogel composite reaches 377 kPa,

which is approximately 2.8 times in comparison to the pure ionogel. Additionally, its Young's modulus of approximately 103.2 kPa is comparable to that of human tissues and lower than 193.1 kPa of the intrinsic ionogel.⁵³ Similarly, the Au NWs ionogel composite achieves a strain of up to 610%, fracture strength at 244 kPa, and Young's modulus of 92.3 kPa (Figure 2b). The GO ionogel composite exhibits a fracture strain, tensile strength, and Young's modulus of 538%, 306 kPa, and approximately 200.5 kPa, respectively (Figure 2b). The improvement of mechanical properties of ionogel nanocomposites may be attributed to (i) the strong interaction between highly cross-linked polymer networks and entangled nanowires or nanofillers, and (ii) dipole interactions between nanofillers and ILs, along with the hydrogen bonds, and iondipole interactions between the functional groups on the polymer matrix and ILs.54,55

Figure 2c-f provides a systematic evaluation of the P(AAm-co-AA) ionogel nanocomposites as resistive strain sensors, indicating that the Ag NWs ionogel composite exhibits the highest sensitivity compared with the other three. The gauge factor (GF), represented by the $\Delta R/R_0$ to strain ratio, is introduced to describe the sensing performance. Figure 2c, is assigned to the relative change of electrical resistance ($\Delta R/R_0$) for the P(AAm-co)

-AA) ionogel nanocomposites as a function of strain. The Ag NWs ionogel composite exhibits GF around 0.13 for the strain ranging from 0% to approximately 75% strain and GF around 0.019 for the strain greater than 75% to fracture, which shows significant improvement in comparison with those of the pure ionogel (the GF values for the two strain regimes are 0.077 and 8.6×10^{-3} , respectively, Figure S5a,b, Supporting Information). Figure 2d shows the resistive change of a slab of the Ag NW ionogel composite during cyclic testing

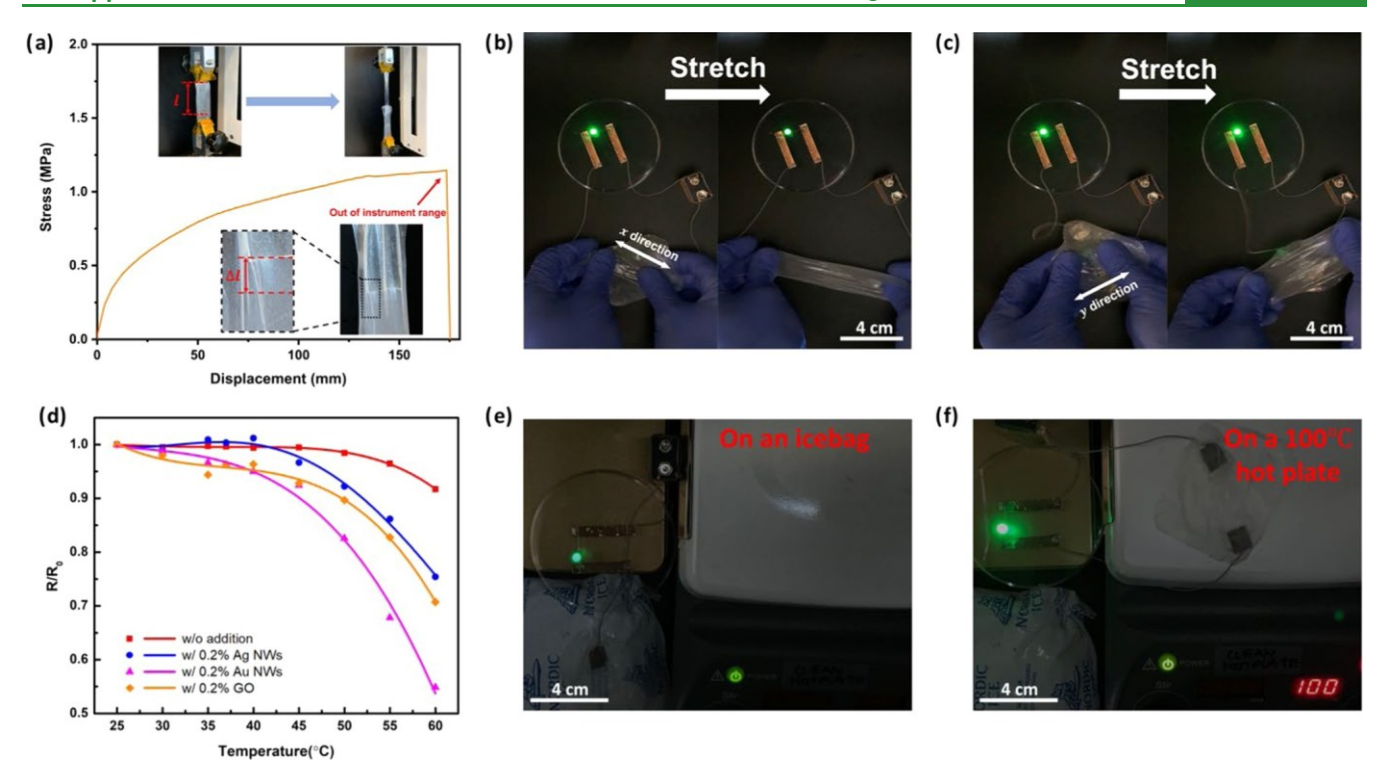


Figure 3. Thermal property and adhesive characterization of ionogel nanocomposites. (a) Measured stress by pulling a polyurethane slab (48 mm \times 27 mm \times 0.2 mm, length \times width \times thickness) from an adhered slab (38 mm \times 15 mm \times 0.4 mm, length \times width \times thickness) of Ag NWs ionogel composite as a function of pulling displacement. The initial adhesion area is 570 mm². (b, c) Optical images showing the brightness change of a green LED light caused by stretching the fabricated ionogel-Ag NWs composite strain sensor along the longitudinal (b) and transverse (c) directions, respectively. (d) Measured resistive change of R/R_0 of ionogel nanocomposites as a function of temperature. (e, f) Optical images of the brightness change of a green LED lamp due to the temperature change of the strain sensor achieved by transferring it from an icebag (e) to a 100 °C hot plate (f).

under a series of small strains (1, 2, 5, and 10%), indicating good sensing stability and accuracy.

Figure 2e shows the performance of the Ag NWs ionogel composite in comparison with the Au NWs ionogel composite, GO ionogel composite, and pure ionogel under repeated stretching to 10% strain. The Ag NWs ionogel composite exhibits higher sensitivity compared with that of the other ionogel composites and the pure ionogel. The improvement of the electrical properties using a very small amount of Ag NWs again demonstrates the feasibility of a strategy to further improve the sensing properties of conductive ionogels through conductive fillers. The increased sensitivity can be attributed to the superior conductivity of Ag NWs, which significantly augments the electron transmission capabilities of the sensor. During the stretching of the sensor, the originally staggered nanowires within the ionogel polymer network are compelled to disengage from their initial contact positions or stacked configurations due to elongation of the polymer chains, which further results in an associated increase in resistance. Figure 2f shows the experimental results on a strain sensor based on the Ag NWs ionogel composite in response to various loading weights. The results reveal that increasing the loading weight led to a consistent linear increase of both the deformation (from 0 to 12 mm) and relative resistance (from 0 to 2.4 k Ω) of the sensor, indicating its promising potential to serve as a wearable strain sensor.

To leverage the advantageous properties of the Ag NWs ionogel composite in constituting wearable strain sensors, we use two layers of PU films (Houseables) (Figure S4) to fully encapsulate the Ag NWs ionogel composite. Such an

encapsulation strategy effectively prevents leakage of the ILs, allows good adhesion between the sensor and skin, and improves the biocompatibility of the device without compromising its sensing performance. Figure 3a illustrates the good adhesion between the Ag NWs ionogel composite and the PU film, confirming its robust integration. As shown in Figure 3a, applying a stress of 1.15 MPa leads to a high stretch deformation of approximately 174 mm (ca. 458% strain) but a relatively small shift displacement (4 mm, ~10.5% of the stretch deformation) between the two bonded layers (PU layer and the Ag NWs ionogel composite), suggesting their good adhesion without compromising high stretchability. Figure 3b,c provides a visualized demonstration of the strain responsivity of the Ag NWs ionogel composite sensor by connecting it with a light-emitting diode (LED) powered by a battery. The sensor is in a slab shape in which the two ends along the longitudinal direction (defined as the x direction in Figure 3b) connect into LED circuits (Figure S8). As shown in Figure 3b,c, stretching along the *x* direction results in a significant decrease in the brightness of the LED, while stretching along the *y* direction leads to an observable increase in the brightness of the LED. This observation on the change of LED brightness can be explained by the following resistance equation that dictates the resistive behavior of the Ag NWs ionogel composite sensor.

$$R = \frac{\rho L}{A}$$

where R is the resistance of the conductor, ρ is the resistivity of the conductor, L is the length, and A is the cross-sectional area of the slab-shaped sensor. Here, stretching along the x

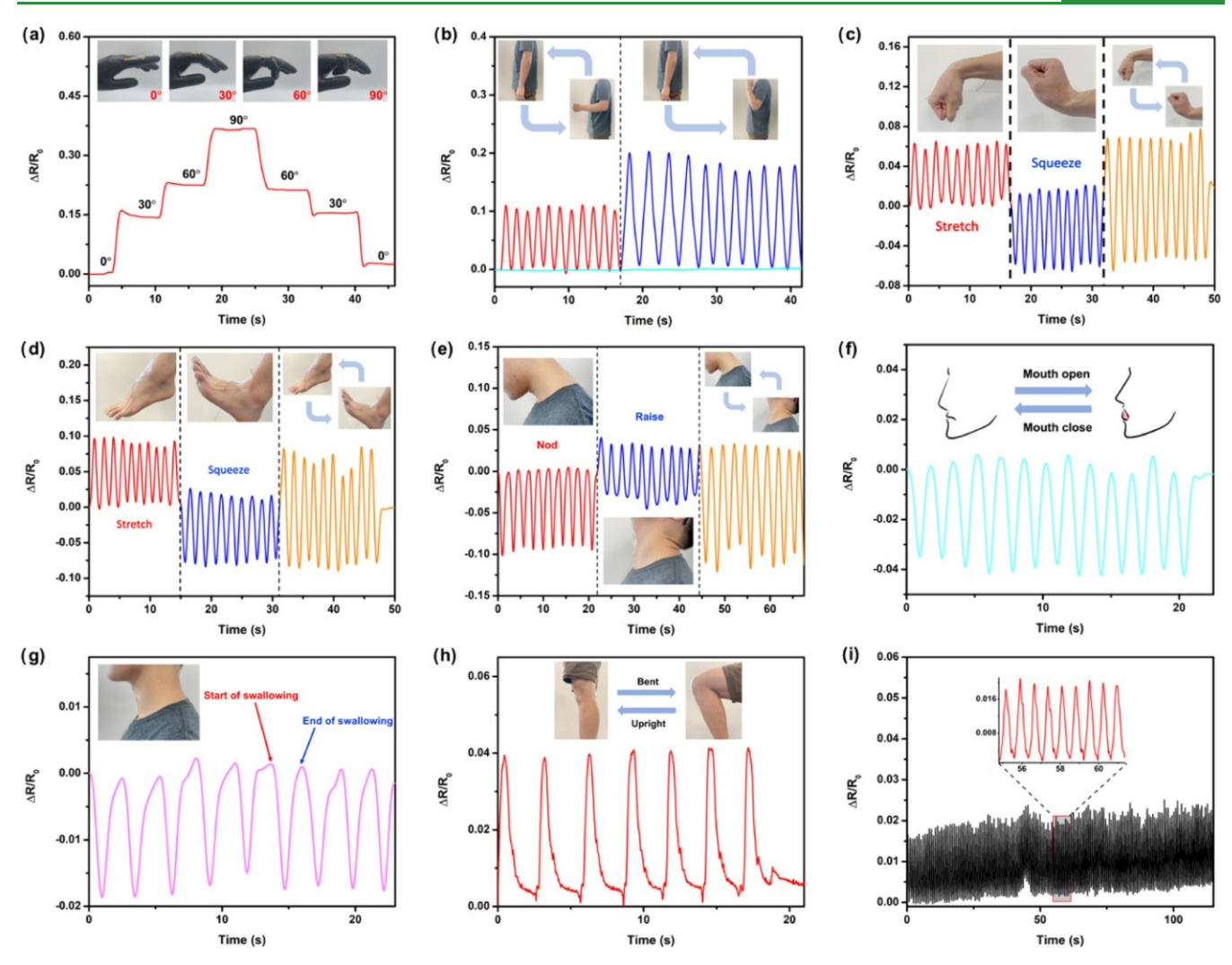


Figure 4. Demonstrations of wearable strain sensors based on Ag NWs ionogel composite for various motion monitoring. (a) The strain sensor is fixed on the knuckles and bent at various angles. (b) The strain sensor is attached to the elbow and repeatedly raises and lowers the forearm to various degrees. (c, d) The strain sensors are placed at the wrist (c) and ankle (d), respectively, that continuously stretch downward and squeeze upward at various angles. (e-g) The strain sensor is placed on the tracheal region of the neck during repeatedly (e) nodding and bending motions, (f) speaking motions, and (g) swallow motions, respectively. (h, i) The strain sensor is attached to the knee that undergoes (h) squat motions and (i) cycling motions, respectively.

direction leads to an increase of L and a decrease of A, thus increasing R, while stretching along the y direction leads to a decrease of L and an increase of A, thus decreasing R. Supporting Video S1 shows the brightness change of the LED in real time in response to the stretch-release processes on the sensor.

Figure 3d shows the temperature-induced modulation of the sensor resistance. Specifically, the results indicate a consistent decrease in resistance for all of the test samples (Ag NWs ionogel composite, Au NWs ionogel composite, GO ionogel composite, and pure ionogel) as temperature increases. For the clinically relevant temperature range between 25 and 40 °C, the R/R_0 values dropped below 1 for the ionogels filled with Au NWs and GO, but remained relatively stable for the pure ionogel and Ag NWs ionogel composite. This suggests that the sensor can remain relatively unaffected by temperature variations within the normal temperature range of the human body. In addition, Figure 3e,f and Supporting Video S2 provide a visualized demonstration of the Ag NWs ionogel composite in response to temperature. Here, the sensor was subjected to

extreme temperature conditions, placed on an icebag at -20 °C, and then transferred to a hot plate at 100 °C, as shown in Figure 3e,f, respectively. The LED connected to the sensor positioned on the hot plate exhibited a significantly higher brightness compared to that placed on the icebag. The temperature-dependent changes in resistance may be attributed to the synergistic effects of ILs and nanofillers. At lower temperatures, the electrical resistance of ILs typically increases due to reduced ion mobility caused by cooling.⁵⁶ Conversely, as the temperature rises, the electrical resistance of ILs generally decreases owing to enhanced ion mobility and change in dielectric constant.⁵⁷ The presence of different nanofillers further alters the charge mobility and dielectric constant possibly through the introduction of electrons within the nanofillers as charge carriers and their interactions with the ions in ILs.58,59

The high stretchability, tissue-like softness, strong strain sensitivity, and acceptable thermal stability of the Ag NWs ionogel composite enable its utility in constructing wearable strain sensors for monitoring human body motions. Figure 4

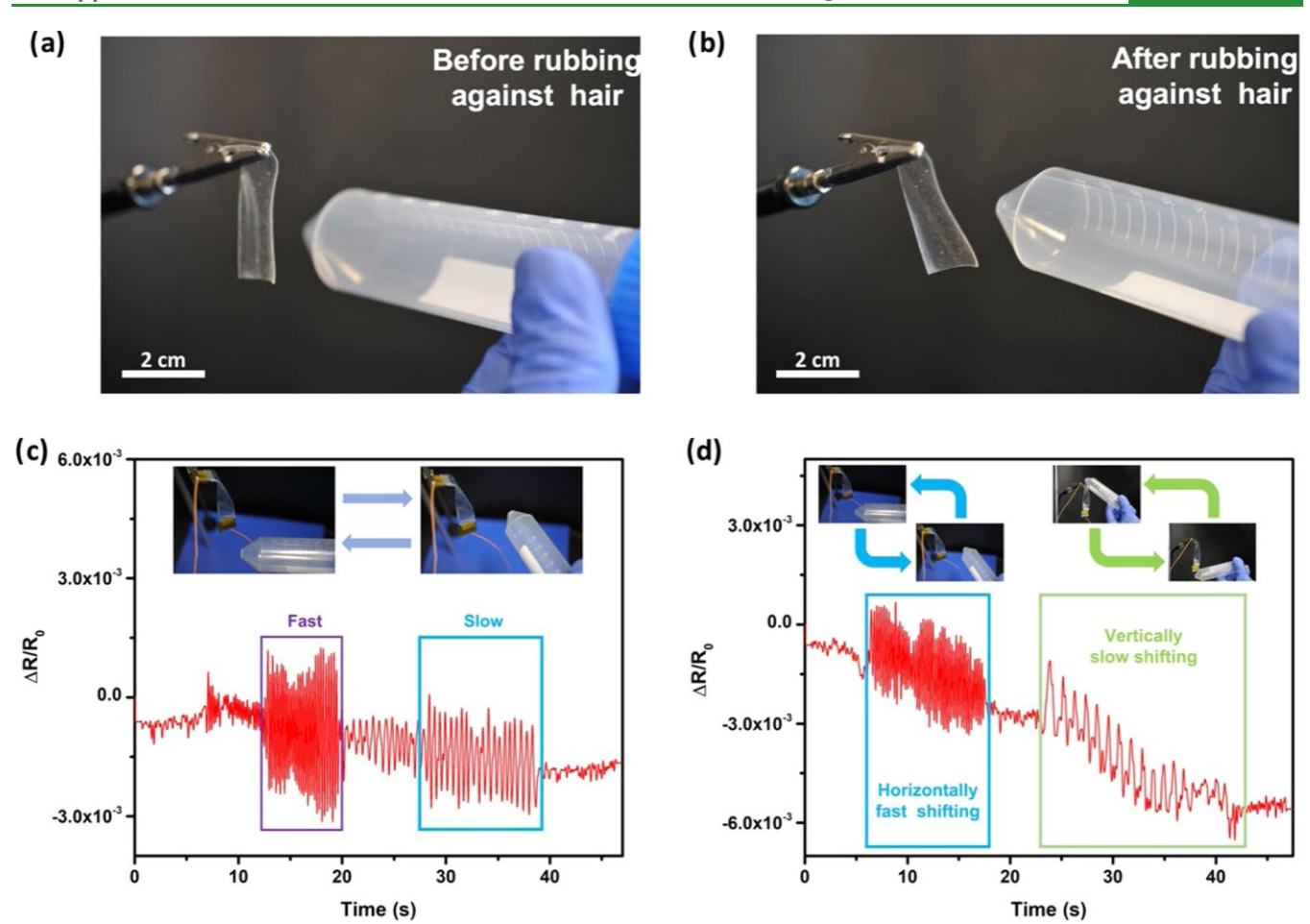


Figure 5. Demonstrations of the robotic motion of the ionogel nanocomposites via electrostatic attraction. Rubbing a plastic tube against hair generates a static charge on the surface, which leads to a strong motion of a slab of the Ag NWs ionogel nanocomposite from a resting state (a) to a bent state (b). Measured resistive change of $\Delta R/R_0$ plots of Ag NWs ionogel composites during the bending motion triggered by the electrostatic attraction. The electrostatically charged tube undergoes (c) a fast and slow horizontal shifting and (d) a fast horizontal shifting followed by a vertically slow shifting.

displays the relative resistance change of a strain sensor based on Ag NWs ionogel composites in response to various situations of body motions. As illustrated in Figure 4a, we prepared a Ag NWs ionogel composite strain sensor (with a gel size of 10 mm \times 5 mm, length x width) and fixed it at the second knuckle of the index finger of a latex glove using commercial tape. the index finger was first taken straight at 0°, and the second knuckle was set as the origin to bend 30, 60, and 90° toward the palm. As the bending angle of the finger became larger, the sensor resistance became larger. When the finger was held at a certain angle, the sensor resistance remained stable with little observable fluctuation. Moreover, the results show no observable hysteresis of sensor resistance during the cyclic bending and unbending movement, indicating high sensing reproducibility and accuracy. We further attached the sensor to the elbow with PU transparent film dressings, as shown in Figure 4b. The starting position was set with the arm hanging vertically, and the red line represents the signal variation resulting from the forearm bending upward and downward around 90°, with the elbow as the origin. The blue line represents the sensing signal variation when the forearm was bent upward until its bending limitation. The cyan line represents the sensing signal variation during the stationary state (starting position). The results indicate that the sensor exhibits excellent real-time responsiveness without

obvious hysteresis during practical usage. Furthermore, the cyan line maintained a relatively constant level, showing good stability of the strain sensor during the stationary state. We also performed motion monitoring on highly flexible body parts such as wrist, ankle, and neck and then demonstrated its excellent sensing performance. In Figure 4c, the starting position was set with the fist and forearm maintained in a horizontal position. When the wrist bent downward, the sensor was stretched, leading to an increase in the sensor resistance, which decreased upon returning to the initial position. Conversely, when the wrist bent upward, the sensor was squeezed, and the sensor resistance decreased. In addition, the orange line in Figure 4d represents the sensing signal variation from the lower bending limit to the upper bending limit of the wrist. The results further demonstrate the accurate monitoring capability of the strain sensor based on the Ag NWs ionogel composite. Moreover, the sensor shows excellent strain monitoring on the ankle as demonstrated in Figure 4d. As the foot tightened downward, the sensor resistance increased, while it decreased when the foot was lifted upward. In Figure 4e, the sensor was placed on the neck near the tracheal region. When the head nodded downward, the sensor experienced compression, leading to a decrease in sensor resistance, while the sensor resistance increased as the head tilted upward. Furthermore, the sensor placed on the neck can monitor

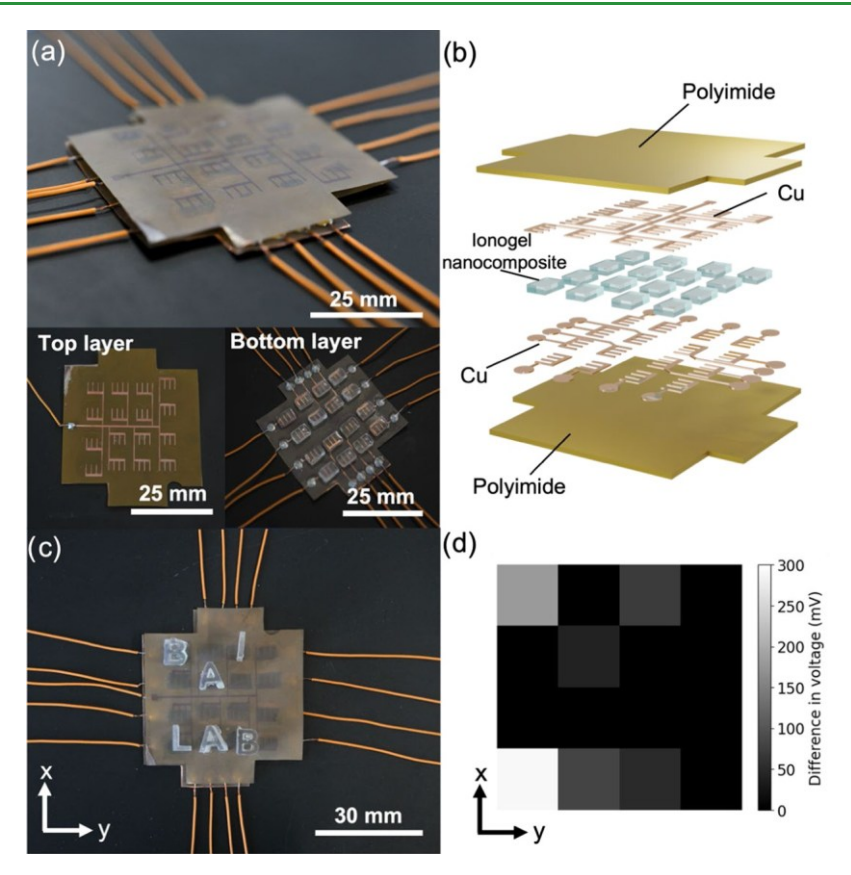


Figure 6. Flexible pressure sensor array based on the Ag NW ionogel composite. (a) Optical image of the 4×4 sensor pixel arrays to detect pressure distribution. (b) Corresponding schematic illustration showing the exploded view of the pixel array. (c) Six letter blocks made by 3D printing were placed on the sensor arrays. (d) Measured corresponding output at each pixel. The color contrast of each pixel shows local pressure distribution that is in agreement with the respective positions of the letter blocks.

mouth movements (mouth opening and swallowing) as well (Figure 4f,g). The results in Figure 4f show good correspondence with the mouth movement, where the peaks and valleys indicate mouth opening and closing, respectively. The swallowing test, as shown in Figure 4g, monitored a repeated process of water intake, indicating a good response of the strain sensor to the throat movement. Furthermore, we also attached the sensor to the knee to monitor leg lifting movements (Figure 4h). The test similarly displayed real-time monitoring and an excellent response speed. The minor hysteresis of the strain sensor can be observed during the recovery process, which is possibly due to the imperfect adhesion of the sensor to the knee, which leads to a small shift in the relative position. This phenomenon can be eliminated by increasing sensor sizes and strengthening the sensor adhesion with a clinical-grade Tegaderm. The performance of the strain sensor during intense physical activity was evaluated through a 2 min cycling experiment on a stationary exercise bike. The monitoring signals of the right knee shown in Figure 4i revealed a relatively stable variation of the sensor resistance during exercise. From the partial zoomed-in view in Figure 4i, the response sensitivity and reproducibility of the strain sensor in relation to the exercise intensity were not significantly affected, which was attributed to the improved stability supported by the PU dressing to the Ag NWs ionogel composite. In order to further characterize the stability, we also conducted thorough tests simulating real-world usage conditions throughout different seasons, times of the day and using scenarios, such as water, some solvents, and other

substances commonly encountered in daily life. We observed no issues related to instability or malfunction in the sensors during testing. Moreover, combined with its excellent adhesion to skin, it ensures consistent and accurate monitoring of the user's movements, adding to the overall reliability of the sensor devices.

In addition, the Ag NWs ionogel composite demonstrated a strong response to an external electric field. One end of the composite was fixed to a steel clamp, and one plastic tube that had not been rubbed against hair and another that had been rubbed against hair were approached near the lower end of the composite as shown in Figure 5a,b. The positive charges caused the ionogel to be attracted toward the tube. This is due to the presence of an electric field around the plastic tube, which was formed by the charged particles on the tube surface. The charged tube and the ionogel experienced a charge difference due to the ability of polarization of the ionogel, resulting in an electrostatic force that drives the ionogel to move toward the plastic tube (Video S3, Supporting Information). To observe and record the effects of the external electric field on the Ag NWs ionogel composite more clearly, the composite was connected to an electrical circuit and the charged plastic tube was shifted back and forth near it. As shown in Figure 5c, during rapid shifts, there were intense and drastic variations in the sensing signal. When the swings were performed with almost the same amplitude but at a slow speed, the sensing signal weakened and became more sporadic compared to the fast shifts. To investigate the directional dependence of the shift, the sensor resistance measured during

vertical shifts was compared to those measured during horizontal shifts, as shown in Figure 5d. The results exhibited a larger response for vertical shifts. In comparison, no motions have been observed from several conventional elastomers (e.g., PDMS and Eco-flex) with the same size as the slab of ionogel nanocomposite for the same experiment (Video S3, Supporting Information).

To further explore the potential of the Ag NWs ionogel nanocomposite for applications in wearable sensors, we fabricated a 4×4 pressure sensor array where the incorporated ionogel nanocomposite serves as a piezoresistive interface to generate resistive responses to the spatial distribution of external pressure, as shown in Figure 6a. Here, the ionogel nanocomposites used in our pressure sensor were not encapsulated individually due to the presence of copper loops on the top and bottom polyimide films of the sensor device. Figure 6b displays an exploded view of the device, where the interdigitated electrodes are utilized to define the vertical orientation force and limit the interference with each resistance valve, respectively. In comparison with the pristine resistance output, the capacitance efficacy of each sensing pixel was also taken into consideration. Thus, the designed impedance converter circuit (Figures S10[TC13] and S11) was subsequently connected to the array, integrating the capacitance and resistance for higher sensing accuracy. When six letters were placed on the surface of the sensor arrays (Figure 6c), the distributions at each pixel were recorded and measured, as shown in Figure 6d. The color contrast mapping was consistent with that of the corresponding positions. The contrast difference in the map can reveal the weight of varied letters, attributed to the ionogel-Ag NWs composite interlayer. Consequentially, the highly stretchable and tissue-like gel is sensitive to changes in the external electric field and exogenous stress, indicating the promising potential applications of this material in fields such as biomedical technology and health monitoring.

CONCLUSIONS

In this work, we introduce the development of a highly stretchable, tissue-like strain sensor for monitoring body movements. The sensor is based on a composite of a P(AAm-co-AA) ionogel and Ag NWs. It exhibits high stretchability of up to 605% and strength at a break of 377 kPa. In addition to its excellent performance as a strain sensor in practical tests on the human body, it also demonstrates sensitive responses to high temperatures and electrostatic attraction. By encapsulating it in PU transparent film dressings, we not only solve the issue of potential irritation to the human skin but also achieve strong adhesion between the composite and dressings, enabling multidirectional stretching sensing and therefore broadening its detection and application range. The strain sensor based on the Ag NWs ionogel composite exhibits outstanding body monitoring, stability, and repeatability performance. Beyond this, the fabricated pressure sensor array demonstrated its ability to distribute stress and detect variations in external electric fields and stress. We believe that with further research and optimization, it can have more promising applications in wearable and flexible strain sensor fields, among others.

ASSOCIATED CONTENT

Data Availability Statement

All data needed to evaluate the conclusions in the paper are present in the paper and/or the Supporting Information.

***** Supporting Information

The Supporting Information is available free of charge at https://pubs.acs.org/doi/10.1021/acsami.4c10539.

Experimental synthesis and supporting morphology of ionogels and fillings; fabrication of ionogel-composited wearable strain sensor; characterization of mechanical, optical, and electrical properties of devices; and signal conditioning circuit design for impedance conversion of the ionogel-composited devices (PDF)

Brightness change of the LED in real time (Video S1) (MP4)

Visualized demonstration of the Ag NWs ionogel composite (Video S2) (MP4)

Electrostatic force that drives the ionogel to move toward the plastic tube (Video S3) (MP4)

AUTHOR INFORMATION

Corresponding Author

Wubin Bai — Department of Applied Physical Science, University of North Carolina at Chapel Hill, Chapel Hill, North Carolina 27514, United States; Email: wbai@ unc.edu

Authors

Siyuan Liu — Department of Applied Physical Science, University of North Carolina at Chapel Hill, Chapel Hill, North Carolina 27514, United States

Yizhang Wu — Department of Applied Physical Science, University of North Carolina at Chapel Hill, Chapel Hill, North Carolina 27514, United States; ⊚ orcid.org/0000-0001-6244-8458

Lai Jiang — Department of Biology, University of North Carolina, Chapel Hill, North Carolina 27514, United States

Wanrong Xie − Department of Applied Physical Science, University of North Carolina at Chapel Hill, Chapel Hill, North Carolina 27514, United States; orcid.org/0009-0001-5872-1228

Brayden Davis – Joint Department of Biomedical Engineering, University of North Carolina at Chapel Hill & North Carolina State University, Chapel Hill, North Carolina 27514, United States; orcid.org/0009-0002-8155-7152

Meixiang Wang — Department of Chemical and Biomolecular Engineering, North Carolina State University, Raleigh, North Carolina 27606, United States; ⊙ orcid.org/0000-0001-8441-2288

Lin Zhang — Department of Applied Physical Science, University of North Carolina at Chapel Hill, Chapel Hill, North Carolina 27514, United States

Yihan Liu — Department of Applied Physical Science, University of North Carolina at Chapel Hill, Chapel Hill, North Carolina 27514, United States

Sicheng Xing – Joint Department of Biomedical Engineering, University of North Carolina at Chapel Hill & North Carolina State University, Chapel Hill, North Carolina 27514, United States

Michael D. Dickey — Department of Chemical and Biomolecular Engineering, North Carolina State University, Raleigh, North Carolina 27606, United States; o orcid.org/0000-0003-1251-1871

Complete contact information is available at: https://pubs.acs.org/10.1021/acsami.4c10539

Author Contributions

¹S.L. and Y.W. contributed equally to this work. S.L. and W.B. conceived the idea. W.B. supervised the project. S.L. carried out most of the experiments. Y.W. participated in the pressure sensor fabrication and measurements. L.J., B.D., and M.W. participated in the ionogel nanocomposite synthesis. L.Z. contributed to the mechanical measurements. W.X. participated in the SEM measurements. Y.L. and S.X. contributed to the data processing and analysis. S.L., M.D.D., and W.B. wrote the paper, and all authors reviewed the manuscript.

Notes

The authors declare no competing financial interest.

ACKNOWLEDGMENTS

This work was supported by start-up funds from the University of North Carolina at Chapel Hill and the fund from the National Science Foundation (award no. ECCS-2139659). The authors also acknowledge the support from the NC Translational and Clinical Sciences (NC TraCS) Institute, which is supported by the National Center for Advancing Translational Sciences (NCATS), National Institutes of Health, through Grant Award Number UL1TR002489. This work was performed in part at the Chapel Hill Analytical and Nanofabrication Laboratory, CHANL, a member of the North Carolina Research Triangle Nanotechnology Network, RTNN, which is supported by the National Science Foundation, Grant ECCS-2025064, as part of the National Nanotechnology Coordinated Infrastructure, NNCI. Research reported in this publication was also supported by the National Institute of Biomedical Imaging and Bioengineering at the National Institutes of Health under award number 1R01EB034332-01.

REFERENCES

- (1) Niu, Y.; Liu, H.; He, R.; Li, Z.; Ren, H.; Gao, B.; Guo, H.; Genin, G. M.; Xu, F. The New Generation of Soft and Wearable Electronics for Health Monitoring in Varying Environment: From Normal to Extreme Conditions. *Mater. Today* 2020, *41*, 219–242.
- (2) Mamun, M. A. Al.; Yuce, M. R. Sensors and Systems for Wearable Environmental Monitoring Toward IoT-Enabled Applications: A Review. *IEEE Sens. J.* 2019, *19* (18), 7771–7788.
- (3) Butt, M. A.; Kazanskiy, N. L.; Khonina, S. N. Revolution in Flexible Wearable Electronics for Temperature and Pressure Monitoring □ A Review. *Electronics* 2022, *11* (5), 716.
- (4) Arman Kuzubasoglu, B.; Kursun Bahadir, S. Flexible Temperature Sensors: A Review. *Sens. Actuators*, A 2020, 315, No. 112282.
- (5) Zazoum, B.; Batoo, K. M.; Khan, M. A. A. Recent Advances in Flexible Sensors and Their Applications. *Sensors* 2022, *22* (12), 4653.
- (6) Pyo, S.; Lee, J.; Bae, K.; Sim, S.; Kim, J. Recent Progress in Flexible Tactile Sensors for Human-Interactive Systems: From Sensors to Advanced Applications. *Adv. Mater.* 2021, *33*, No. 2005902.
- (7) Yang, J. C.; Mun, J.; Kwon, S. Y.; Park, S.; Bao, Z.; Park, S. Electronic Skin: Recent Progress and Future Prospects for Skin-Attachable Devices for Health Monitoring, Robotics, and Prosthetics. *Adv. Mater.* 2019, *31*, No. 1904765.
- (8) Nie, B.; Liu, S.; Qu, Q.; Zhang, Y.; Zhao, M.; Liu, J. Bio-Inspired Flexible Electronics for Smart E-Skin. *Acta Biomater*. 2022, *139*, 280–295.

- (9) Chen, G.; Li, Y.; Bick, M.; Chen, J. Smart Textiles for Electricity Generation. *Chem. Rev.* 2020, *120* (8), 3668–3720.
- (10) Chen, G.; Xiao, X.; Zhao, X.; Tat, T.; Bick, M.; Chen, J. Electronic Textiles for Wearable Point-of-Care Systems. *Chem. Rev.* 2022, *122* (3), 3259–3291.
- (11) Libanori, A.; Chen, G.; Zhao, X.; Zhou, Y.; Chen, J. Smart Textiles for Personalized Healthcare. *Nat. Electron.* 2022, *5*, 142–156.
- (12) Yin, J.; Wang, S.; Di Carlo, A.; Chang, A.; Wan, X.; Xu, J.; Xiao, X.; Chen, J. Smart Textiles for Self-Powered Biomonitoring. *Med-X* 2023, *I* (1), 3 DOI: 10.1007/s44258-023-00001-3.
- (13) Shen, Y.; Wang, Y.; Luo, Z.; Wang, B. Durable, Sensitive, and Wide-Range Wearable Pressure Sensors Based on Wavy-Structured Flexible Conductive Composite Film. *Macromol. Mater. Eng.* 2020, 305 (8), No. 2000206.
- (14) Zhu, Y.; Xu, F.; Wang, X.; Zhu, Y. Wavy Ribbons of Carbon Nanotubes for Stretchable Conductors. *Adv. Funct. Mater.* 2012, 22 (6), 1279–1283.
- (15) Yu, H. C.; Hao, X. P.; Zhang, C. W.; Zheng, S. Y.; Du, M.; Liang, S.; Wu, Z. L.; Zheng, Q. Engineering Tough Metallosupramolecular Hydrogel Films with Kirigami Structures for Compliant Soft Electronics. *Small* 2021, *17* (41), No. 210836.
- (16) Ning, X.; Wang, X.; Zhang, Y.; Yu, X.; Choi, D.; Zheng, N.; Kim, D. S.; Huang, Y.; Zhang, Y.; Rogers, J. A. Assembly of Advanced Materials into 3D Functional Structures by Methods Inspired by Origami and Kirigami: A Review. *Adv. Mater. Interfaces* 2018, *5* (13), No. 1800284
- (17) Meng, K.; Xiao, X.; Liu, Z.; Shen, S.; Tat, T.; Wang, Z.; Lu, C.; Ding, W.; He, X.; Yang, J.; Chen, J. Kirigami-Inspired Pressure Sensors for Wearable Dynamic Cardiovascular Monitoring. *Adv. Mater.* 2022, *34* (36), No. 2202478.
- (18) Huyghe, B.; Rogier, H.; Vanfleteren, J.; Axisa, F. Design and Manufacturing of Stretchable High-Frequency Interconnects. *IEEE Trans. Adv. Packag.* 2008, *31* (4), 802–808.
- (19) Zamarayeva, A. M.; Ostfeld, A. E.; Wang, M.; Duey, J. K.; Deckman, I.; Lechêne, B. P.; Davies, G.; Steingart, D. A.; Arias, A. C. Flexible and Stretchable Power Sources for Wearable Electronics. *Sci. Adv.* 2017, *3* (6), No. e1602051.
- (20) Zhang, Y.; Xu, S.; Fu, H.; Lee, J.; Su, J.; Hwang, K. C.; Rogers, J. A.; Huang, Y. Buckling in Serpentine Microstructures and Applications in Elastomer-Supported Ultra-Stretchable Electronics with High Areal Coverage. *Soft Matter* 2013, *9* (33), 8062–8070.
- (21) Miyamoto, A.; Lee, S.; Cooray, N. F.; Lee, S.; Mori, M.; Matsuhisa, N.; Jin, H.; Yoda, L.; Yokota, T.; Itoh, A.; Sekino, M.; Kawasaki, H.; Ebihara, T.; Amagai, M.; Someya, T. Inflammation-Free, Gas-Permeable, Lightweight, Stretchable on-Skin Electronics with Nanomeshes. *Nat. Nanotechnol.* 2017, *12* (9), 907–913.
- (22) Wang, J.; Wu, B.; Wei, P.; Sun, S.; Wu, P. Fatigue-Free Artificial Ionic Skin Toughened by Self-Healable Elastic Nanomesh. *Nat. Commun.* 2022, *13* (1), No. 4411.
- (23) Shintake, J.; Piskarev, E.; Jeong, S. H.; Floreano, D. Ultrastretchable Strain Sensors Using Carbon Black-Filled Elastomer Composites and Comparison of Capacitive Versus Resistive Sensors. *Adv. Mater. Technol.* 2018, *3* (3), No. 1700284.
- (24) Chakraborty, P.; Guterman, T.; Adadi, N.; Yadid, M.; Brosh, T.; Adler-Abramovich, L.; Dvir, T.; Gazit, E. A Self-Healing, All-Organic, Conducting, Composite Peptide Hydrogel as Pressure Sensor and Electrogenic Cell Soft Substrate. *ACS Nano* 2019, *13* (1), 163–175.
- (25) Chen, J.; Yu, Q.; Cui, X.; Dong, M.; Zhang, J.; Wang, C.; Fan, J.; Zhu, Y.; Guo, Z. An Overview of Stretchable Strain Sensors from Conductive Polymer Nanocomposites. *J. Mater. Chem. C* 2019, 7, 11710—11730
- (26) Oh, J. Y.; Son, D.; Katsumata, T.; Lee, Y.; Kim, Y.; Lopez, J.; Wu, H. C.; Kang, J.; Park, J.; Gu, X.; Mun, J.; Wang, N. G. J.; Yin, Y.; Cai, W.; Yun, Y.; Tok, J. B. H.; Bao, Z. Stretchable Self-Healable Semiconducting Polymer Film for Active-Matrix Strain-Sensing Array. *Sci. Adv.* 2019, *5* (11), No. eaav3097.
- (27) Dickey, M. D. Stretchable and Soft Electronics Using Liquid Metals. *Adv. Mater.* 2017, *29* (17), No. 1606425.

- (28) Pei, D.; Yu, S.; Liu, P.; Wu, Y.; Zhang, X.; Chen, Y.; Li, M.; Li, C. Reversible Wet-Adhesive and Self-Healing Conductive Composite Elastomer of Liquid Metal. *Adv. Funct. Mater.* 2022, *32* (35), No. 2204257.
- (29) Jia, M.; Rolandi, M. Soft and Ion-Conducting Materials in Bioelectronics: From Conducting Polymers to Hydrogels. *Adv. Healthcare Mater.* 2020, *9* (5), No. 1901372.
- (30) Zhao, Y.; Kim, A.; Wan, G.; Tee, B. C. K. Design and Applications of Stretchable and Self-Healable Conductors for Soft Electronics. *Nano Convergence* 2019, *6*, 25.
- (31) Liu, H.; Li, M.; Liu, S.; Jia, P.; Guo, X.; Feng, S.; Lu, T. J.; Yang, H.; Li, F.; Xu, F. Spatially Modulated Stiffness on Hydrogels for Soft and Stretchable Integrated Electronics. *Mater. Horiz.* 2020, 7 (1), 203–213
- (32) Ohm, Y.; Pan, C.; Ford, M. J.; Huang, X.; Liao, J.; Majidi, C. An Electrically Conductive Silver–Polyacrylamide–Alginate Hydrogel Composite for Soft Electronics. *Nat. Electron.* 2021, *4*, 185–192.
- (33) Zhang, Y. S.; Khademhosseini, A. Advances in Engineering Hydrogels. *Science* 2017, *356* (6337), No. aaf3627.
- (34) Yuk, H.; Lu, B.; Zhao, X. Hydrogel Bioelectronics. *Chem. Soc. Rev.* 2019, 48, 1642–1667.
- (35) Yuk, H.; Zhang, T.; Parada, G. A.; Liu, X.; Zhao, X. Skin-Inspired Hydrogel-Elastomer Hybrids with Robust Interfaces and Functional Microstructures. *Nat. Commun.* 2016, 7, No. 12028.
- (36) Zhang, L.; Jiang, D.; Dong, T.; Das, R.; Pan, D.; Sun, C.; Wu, Z.; Zhang, Q.; Liu, C.; Guo, Z. Overview of Ionogels in Flexible Electronics. *Chem. Rec.* 2020, 20 (9), 948–967.
- (37) Calvert, P. Hydrogels for Soft Machines. *Adv. Mater.* 2009, *21* (7), 743–756.
- (38) Zhou, Y.; Wan, C.; Yang, Y.; Yang, H.; Wang, S.; Dai, Z.; Ji, K.; Jiang, H.; Chen, X.; Long, Y. Highly Stretchable, Elastic, and Ionic Conductive Hydrogel for Artificial Soft Electronics. *Adv. Funct. Mater.* 2019, 29 (1), No. 1806220.
- (39) Odent, J.; Wallin, T. J.; Pan, W.; Kruemplestaedter, K.; Shepherd, R. F.; Giannelis, E. P. Highly Elastic, Transparent, and Conductive 3D-Printed Ionic Composite Hydrogels. *Adv. Funct. Mater.* 2017, *27* (33), No. 1701807.
- (40) Ren, Y.; Liu, Z.; Jin, G.; Yang, M.; Shao, Y.; Li, W.; Wu, Y.; Liu, L.; Yan, F. Electric-Field-Induced Gradient Ionogels for Highly Sensitive, Broad-Range-Response, and Freeze/Heat-Resistant Ionic Fingers. *Adv. Mater.* 2021, *33* (12), No. 2008486.
- (41) Wang, M.; Hu, J.; Dickey, M. D. Tough Ionogels: Synthesis, Toughening Mechanisms, and Mechanical Properties-A Perspective. *JACS Au* 2022, 2 (12), 2645–2657.
- (42) Li, T.; Wang, Y.; Li, S.; Liu, X.; Sun, J. Mechanically Robust, Elastic, and Healable Ionogels for Highly Sensitive Ultra-Durable Ionic Skins. *Adv. Mater.* 2020, *32* (32), No. 2002706.
- (43) Zhang, J.; Liu, E.; Hao, S.; Yang, X.; Li, T.; Lou, C.; Run, M.; Song, H. 3D Printable, Ultra-Stretchable, Self-Healable, and Self-Adhesive Dual Cross-Linked Nanocomposite Ionogels as Ultra-Durable Strain Sensors for Motion Detection and Wearable Human-Machine Interface. *Chem. Eng. J.* 2022, *431*, No. 133949.
- (44) Lu, C.; Chen, Y.; Yu, X. Graphene-Enhanced Double-Network Ionogel Electrolytes for Energy Storage and Strain Sensing. *Polym. Bull.* 2023, *80*, 12895–12905.
- (45) Sun, P.; Wang, Y.; Huang, Z.; Yang, X.; Dong, F.; Xu, X.; Liu, H. Limonene-Thioctic Acid-Ionic Liquid Polymer: A Self-Healing and Antibacterial Material for Movement Detection Sensor. *Ind. Crops Prod.* 2022, *189*, No. 115802.
- (46) Dobler, D.; Schmidts, T.; Zinecker, C.; Schlupp, P.; Schäfer, J.; Runkel, F. Hydrophilic Ionic Liquids as Ingredients of Gel-Based Dermal Formulations. *AAPS PharmSciTech* 2016, *17* (4), 923–931.
- (47) Zhang, L. M.; He, Y.; Cheng, S.; Sheng, H.; Dai, K.; Zheng, W. J.; Wang, M. X.; Chen, Z. S.; Chen, Y. M.; Suo, Z. Self-Healing, Adhesive, and Highly Stretchable Ionogel as a Strain Sensor for Extremely Large Deformation. *Small* 2019, *15* (21), No. 1804651.
- (48) Li, H.; Feng, Z.; Zhao, K.; Wang, Z.; Liu, J.; Liu, J.; Song, H. Chemically Crosslinked Liquid Crystalline Poly(Ionic Liquid)s/Halloysite Nanotubes Nanocomposite Ionogels with Superior Ionic

- Conductivity, High Anisotropic Conductivity and a High Modulus. *Nanoscale* 2019, *11* (8), 3689–3700.
- (49) Wang, M.; Zhang, P.; Shamsi, M.; Thelen, J. L.; Qian, W.; Truong, V. K.; Ma, J.; Hu, J.; Dickey, M. D. Tough and Stretchable Ionogels by in Situ Phase Separation. *Nat. Mater.* 2022, *21* (3), 359–365
- (50) Moon, Y. J.; Kang, K. T. Strain-Induced Alignment of Printed Silver Nanowires for Stretchable Electrodes. *Flexible Printed Electron*. 2022, 7 (2), No. 024003.
- (51) Wang, W.; Guo, P.; Liu, X.; Chen, M.; Li, J.; Hu, Z.; Li, G.; Chang, Q.; Shi, K.; Wang, X.; Lei, K. Fully Polymeric Conductive Hydrogels with Low Hysteresis and High Toughness as Multi-Responsive and Self-Powered Wearable Sensors. *Adv. Funct. Mater.* 2024, No. 2316346.
- (52) Zhao, Y.; Li, Z.; Li, Q.; Yang, L.; Liu, H.; Yan, R.; Xiao, L.; Liu, H.; Wang, J.; Yang, B.; Lin, Q. Transparent Conductive Supramolecular Hydrogels with Stimuli-Responsive Properties for On-Demand Dissolvable Diabetic Foot Wound Dressings. *Macromol. Rapid Commun.* 2020, 41 (24), No. 2000441.
- (53) McKee, C. T.; Last, J. Á.; Russell, P.; Murphy, C. J. Indentation versus Tensile Measurements of Young's Modulus for Soft Biological Tissues. *Tissue Eng.*, *Part B* 2011, *17* (3), 155–164.
- (54) Qin, F.; Sun, L.; Chen, H.; Liu, Y.; Lu, X.; Wang, W.; Liu, T.; Dong, X.; Jiang, P.; Jiang, Y.; Wang, L.; Zhou, Y. 54 Cm2 Large-Area Flexible Organic Solar Modules with Efficiency Above 13%. *Adv. Mater.* 2021, *33* (39), No. 2103017.
- (55) Jiang, Y., Zhao, S.; Wang, F.; Zhang, X.; Su, Z. Highly Stretchable Double Network Ionogels for Monitoring Physiological Signals and Detecting Sign Language. *Biosensors* 2024, 14 (5), 227.
- (56) Vila, J.; Ginés, P.; Pico, J. M.; Franjo, C.; Jiménez, E.; Varela, L. M.; Cabeza, O. Temperature Dependence of the Electrical Conductivity in EMIM-Based Ionic Liquids: Evidence of Vogel-Tamman-Fulcher Behavior. *Fluid Phase Equilib.* 2006, 242 (2), 141–146
- (57) Shim, Y.; Kim, H. J. Dielectric Relaxation and Solvation Dynamics in a Room-Temperature Ionic Liquid: Temperature Dependence. *J. Phys. Chem. B* 2013, *117* (39), 11743–11752.
- (58) Sahu, G.; Das, M.; Yadav, M.; Sahoo, B. P.; Tripathy, J. Dielectric Relaxation Behavior of Silver Nanoparticles and Graphene Oxide Embedded Poly(Vinyl Alcohol) Nanocomposite Film: An Effect of Ionic Liquid and Temperature. *Polymers* 2020, *12* (2), 374.
- (59) Zhang, F. F.; Zheng, F. F.; Wu, X. H.; Yin, Y. L.; Chen, G. Variations of Thermophysical Properties and Heat Transfer Performance of Nanoparticleenhanced Ionic Liquids. *R. Soc. Open Sci.* 2019, 6 (4), No. 182040.